

Article

Theoretical Stark Broadening Parameters for UV–Blue Spectral Lines of Neutral Vanadium in the Solar and Metal-Poor Star HD 84937 Spectra

Cristóbal Colón ^{1,*} , María Isabel de Andrés-García ¹, Lucía Isidoro-García ² and Andrés Moya ¹

¹ Department of Applied Physics, E.T.S.I.D. Industrial, Universidad Politécnica de Madrid, Calle Ronda de Valencia 3, 28012 Madrid, Spain; mariaisabel.deandres@upm.es (M.I.d.A.-G.); a.moya@upm.es (A.M.)

² Department of Industrial Chemistry and Polymers, E.T.S.I.D. Industrial, Universidad Politécnica de Madrid, Calle Ronda de Valencia 3, 28012 Madrid, Spain; lucia.isidoro@upm.es

* Correspondence: cristobal.colon@upm.es; Tel.: +34-910677607

Received: 1 September 2020; Accepted: 26 September 2020; Published: 28 September 2020



Abstract: Using Griem’s semi-empirical approach, we have calculated the Stark broadening parameters (line widths and shifts) of 35 UV–Blue spectral lines of neutral vanadium (V I). These lines have been detected in the Sun, the metal-poor star HD 84937, and Arcturus, among others. In addition, these parameters are also relevant in industrial and laboratory plasma. The matrix elements required were obtained using the relativistic Hartree–Fock (HFR) method implemented in Cowan’s code.

Keywords: atomic data; atomic processes; stark broadening

1. Introduction

Chemical elements belonging to the iron group, from Scandium to Zirconium ($Z = 21–30$), are critical for an understanding of nucleosynthesis in different super-nova types. In particular, Vanadium (together with Scandium and Titanium) is produced by explosive silicon burning and oxygen burning in the core-collapse supernova (SN) phase [1]. In recent works, this element has been analyzed in detail, especially in metal-poor stars [2]. In particular, Cowan et al. [3]—and references therein—find a correlation among Scandium, Titanium, and Vanadium in metal-poor stars. Therefore, the interest in Vanadium spectra has increased, and information about them is relevant for improving its abundance determination accuracy.

Among all the effects that have an impact on atomic spectral lines, the knowledge of the broadening and shift produced by charged particles is essential. Accurate measurements of Stark broadening and shift parameters are required to properly analyze astrophysical data. In the case of Vanadium, Manrique et al. [4] have provided experimental information related to the Stark broadening and shift parameters of the spectral lines of ionized Vanadium (V II).

In addition, the neutral Vanadium has been studied in detail. Infrared spectral lines of neutral vanadium (V I)—7363.1, 8027.3, 8255.8, 9037.6 Å, and so on—have been detected in the Solar spectrum, the spectrum of the metal-poor star HD 84937, and the spectrum of Arcturus ([5–7], respectively).

The levels of V I have been the subject of both experimental and theoretical studies. The earliest works were compiled by [8,9]. The most recent works [10–12] were collected in an exhaustive compilation, revision, and expansion of the V I levels that was carried out by Thorne et al. [13].

As this is an element of great interest, there are relatively recent publications in the literature with transition probabilities that are both theoretical and experimental. A critical analysis of these parameters can be found in [14].

A similar situation is found in the case of other parameters: There are excellent works devoted to the level lifetimes. The most recent are those of Hartog et al. [15], Wang et al. [16], and Holmes et al. [17].

However, despite its interest, we have not found data on the parameters of broadening and displacement of the spectral lines of neutral Vanadium by collision with electrons (Stark parameters) in the National Institute of Standards and Technology (NIST) database [18], nor in the Stark-B database [19].

In addition to its astrophysical interest, the role of vanadium in the corrosion protection of alloys of high industrial interest, as in the case of Ti-6Al-4V [20], is well known. In laser-generated plasma in Laser Sock Process (LSP) experiments with samples of the material mentioned above, intense spectral lines of neutral vanadium and single ionized vanadium can be seen [21,22].

Therefore, electron impact line widths and shifts of V I are relevant in the diagnostics of the plasma of stellar atmospheres, but they are also necessary in the analysis of the plasma in industrial processes.

In this work, electron impact line widths and shifts for 35 spectral lines of neutral vanadium have been calculated using a semi-empirical formalism [23]. The parameters are presented at an electron density of 10^{15} cm^{-3} . We have chosen that electron density because of its proximity to the densities that appear in the LSP experiments. To use them with other densities, they must be multiplied by the appropriate factor; the Stark parameters scale proportionally with the electron density in the semi-empirical approximation.

In the next section, we present our theoretical calculations, which, unlike in previous works, have used previous results of other authors. Below, we present our results for several level lifetimes (comparing them with experimental values obtained from the literature) and Stark broadening parameters. Regarding some lines of astrophysical interest, we show their Stark broadening parameters versus temperature in a graphical representation.

2. Materials and Methods

The semi-empirical formalism in which Griem considered the 1958 Baranger formulation [24] uses Equations (1) and (2), where ω_{se} and d represent the Stark line width (half-width at half-maximum, HWHM) and the Stark line shift, respectively, in angular frequency units, E_H is the hydrogen ionization energy, $E=(3/2) kT$ means the energy of the perturbing electron, N_e is the free electron density, and T is the electron temperature. The initial and final levels of the transitions are denoted by i and f , respectively. In these equations, g_{se} and g_{sh} are the effective Gaunt factors proposed by Seaton [25] and Van Regemorter [26], respectively.

$$\omega_{se} \approx 8 \left(\frac{\pi}{3}\right)^{3/2} \frac{\hbar}{m a_0} N_e \left(\frac{E_H}{kT}\right)^{1/2} \left[\sum_{i'} |\langle i' | \vec{r} | i \rangle|^2 g_{se} \left(\frac{E}{\Delta E_{i'}}\right) + \sum_{f'} |\langle f' | \vec{r} | f \rangle|^2 g_{se} \left(\frac{E}{\Delta E_{f'}}\right) \right] \quad (1)$$

$$d \approx -8 \left(\frac{\pi}{3}\right)^{3/2} \frac{\hbar}{m a_0} N_e \left(\frac{E_H}{kT}\right)^{1/2} \left[\sum_{i'} \left(\frac{\Delta E_{i'}}{|\Delta E_{i'}|}\right) |\langle i' | \vec{r} | i \rangle|^2 g_{sh} \left(\frac{E}{\Delta E_{i'}}\right) - \sum_{f'} \left(\frac{\Delta E_{f'}}{|\Delta E_{f'}|}\right) |\langle f' | \vec{r} | f \rangle|^2 g_{sh} \left(\frac{E}{\Delta E_{f'}}\right) \right] \quad (2)$$

The expression $\Delta\lambda = \omega_{se}\lambda^2/\pi c$ was used to convert the units of angular frequency (obtained in Griem's expressions) into wavelength units. In this equation, $\Delta\lambda$ is the Stark broadening (full-width at half maximum, FWHM), λ is the wavelength, and c is the light speed.

Cowan's Code [27] was used to obtain the necessary matrix elements included in the Equations (1) and (2). This code is a relativistic Hartree–Fock (HFR) approach that uses an intermediate coupling scheme (IC). It allows us to get a complete set of transition probabilities (A_{ij}) of the V I spectral lines by obtaining through them the required matrix elements.

Since the neutral vanadium is an element with a large number of known levels (346 odd levels and 198 even levels in the previously cited work [13]), we preferred not to repeat the very tedious calculations that had already been carried out successfully by this last author Thorne et al. [13]. We used the energies from Thorne et al. [13] and the transition probabilities from Cowan's code to determine the necessary matrix elements in Equations (1) and (2).

The calculations of the present authors were made using the following configurations: even parity, $3d^34s^2 + 3d^44s + 3d^45s + 3d^46s + 3d^44d + 3d^45d + 3d^5 + 3d^34s5s + 3d^34s6s + 3d^34s4d + 3d^34s5d + 3d^34p^2$, and odd parity, $3d^44p + 3d^45p + 3d^34s4p + 3d^34s5p + 3d^44f + 3d^34s4f + 3d^24s^24p$. The atomic parameters that were derived from these calculations and that were used (as input) in our work can be found in Table 6 of Thorne et al. [13].

As there are no previous experimental or theoretical data on the Stark broadening parameters of the spectral lines of the V I, we can only compare atomic data without the effects of the plasma environment, i.e., the intermediate results obtained for the transition probabilities or the level lifetimes. In this case, there are a lot of spectral lines with experimental transition probabilities to include in the comparison (which was made successfully) in our text. We preferred to test the lifetimes of the upper levels of the 35 spectral lines that we considered.

3. Results

Our results for the lifetimes of the upper levels corresponding to the 35 spectral lines with the Stark broadening parameters calculated in this work are presented in Table 1. The first three columns show the level energy, the configuration (as it appears in the NIST databases: using spin-orbit coupling notation and keeping the component with the highest weight), and the wavelengths of the transitions studied. The remaining columns show the values of the experimental level lifetimes found in the literature and the theoretical values obtained in our calculations.

As can be seen, the theoretical values obtained are close to the experimental values, with the noticeable exception of the lifetime value of $3d^44p^4I_{9/2}^o$, which is experimentally (25.8 ns) a factor of two greater than the theoretical value (12.37 ns) obtained in our calculations. This result contrasts with the results obtained for levels of the same multiplet, such as the $3d^44p^4I_{15/2}^o$ level, in which the results obtained are 12.3 and 11.9 ns, respectively.

A possible explanation is found by observing the theoretical values obtained with Cowan's code (ab initio) before adjusting the parameters with the experimental values of the energy levels. For the level $3d^44p^4I_{9/2}^o$, 17.04 ns was obtained, and for the level $3d^44p^4I_{15/2}^o$, 13.85 ns was obtained. This is a known effect: In this case, the energy-optimized Cowan method produces an undesired effect on the result of the transition probabilities for level $3d^44p^4I_{9/2}^o$. It is clearly observed that, in the $37,285 \text{ cm}^{-1}$ level, the relative weight of the vectors (in the spin-orbit coupling notation) $3d^44p^4I_{9/2}^o$, $3d^44p^2H_{9/2}^o$ and $3d^34s4p^2H_{9/2}^o$ changes slightly when adjustments have been made to the experimental levels, significantly affecting the level lifetime.

However, as noted above, our results for the transition probabilities and the oscillator strengths are close to the experimental results in almost all the experimental spectral lines. Stark broadening calculations that depend on all transition probabilities (as can be seen from Equations (1) and (2)) will certainly reflect this effect beyond the effect of any particular transition probability.

Our results for the Stark broadening parameters calculated in this work are presented in Table 2. The first column presents the wavelength and the experimental transition probability of the spectral line. Columns two and three present the transition levels' configurations. The remaining columns show the Stark line widths and shifts at 5, 10, 20 and $30 \cdot 10^3 \text{ K}$ and at an electron density of 10^{15} cm^{-3} . It should be noted that Stark's change parameters could be poorly evaluated. This is due to the fact that the different addends in Equation (2) sometimes carry different signs and are, therefore, very sensitive to possible inaccuracies in the calculations of the matrix elements. This does not happen with the Stark magnification parameter when all terms are positive.

Table 1. Lifetimes of upper levels corresponding to spectral lines with the Stark broadening parameters calculated in this work.

Energy Level (cm ⁻¹) ^a	Configuration	Wavelength in Å ^a	Lifetimes (ns)		
			Expt. ^b	Expt. ^c	This Work
28,368	3d ³ 4s4p ⁶ D _{3/2} ^o	3823.21	35.9		37.8
29,202	3d ³ 4s4p ⁶ P _{3/2} ^o	3690.27	6.7		10.0
		3695.86			
		3705.03			
29,296	3d ³ 4s4p ⁶ P _{5/2} ^o	3692.21 3704.69	6.7	6.9(5)	10.0
29,418	3d ³ 4s4p ⁶ P _{7/2} ^o	3688.06	6.7	7.0(5)	9.98
32,846	3d ³ 4s4p ⁴ F _{5/2} ^o	3056.33	4.1		4.78
32,988	3d ³ 4s4p ⁴ F _{7/2} ^o	3060.45	4.2		4.79
		4095.47			
40,001	3d ³ 4s4p ⁴ G _{9/2} ^o	3207.40	3.3		5.3
43,706	3d ³ 4s4d ⁶ H _{7/2}	3667.73	5.9		6.4
24,648	3d ⁴ 4p ⁶ P _{3/2} ^o	4444.20	28.4		22.2
24,770	3d ⁴ 4p ⁴ P _{1/2} ^o	4412.14	24.7	24(1)	23.6
24,830	3d ⁴ 4p ⁶ F _{3/2} ^o	4400.57	9.2		10.4
		4421.56			
24,838	3d ⁴ 4p ⁶ P _{7/2} ^o	4419.93	28.1		22.5
		4437.83			
24,898	3d ⁴ 4p ⁶ F _{5/2} ^o	4408.19	9.1		10.38
25,253	3d ⁴ 4p ⁶ F _{11/2} ^o	4379.23	9.0		10.26
26,122	3d ⁴ 4p ⁴ F _{7/2} ^o	4182.58	18.0		14.2
26,249	3d ⁴ 4p ⁴ D _{3/2} ^o	3808.51	12.5		13.5
26,397	3d ⁴ 4p ⁶ D _{1/2} ^o	4116.55	8.2		9.1
26,505	3d ⁴ 4p ⁶ D _{5/2} ^o	4105.16	8.1		9.0
		4116.47			
26,604	3d ⁴ 4p ⁶ D _{7/2} ^o	4099.78	8.0		9.1
		4115.17			
26,738	3d ⁴ 4p ⁶ D _{9/2} ^o	4111.78	8.0		9.1
38,115	3d ⁴ 4p ⁴ D _{7/2} ^o	3400.39	5.5		6.5
		3533.67			
37,285	3d ⁴ 4p ⁴ I _{9/2} ^o	4468.00	25.8		12.37
37,518	3d ⁴ 4p ⁴ I _{15/2} ^o	4452.00	12.3		11.9
37,644	3d ⁴ 4p ⁴ G _{9/2} ^o	4560.71	12.3		13.9
39,391	3d ⁴ 4p ⁴ F _{9/2} ^o	4232.45	9.5	5.7(4)	8.0
41,860	3d ⁴ 4p ⁴ G _{9/2} ^o	4050.95	7.5		7.3

^aNIST, ^bHartog et al. [15], ^cWang et al. [16].

As an example, we present the Stark broadening parameters versus temperature for three intense spectral lines of neutral vanadium in Figure 1.

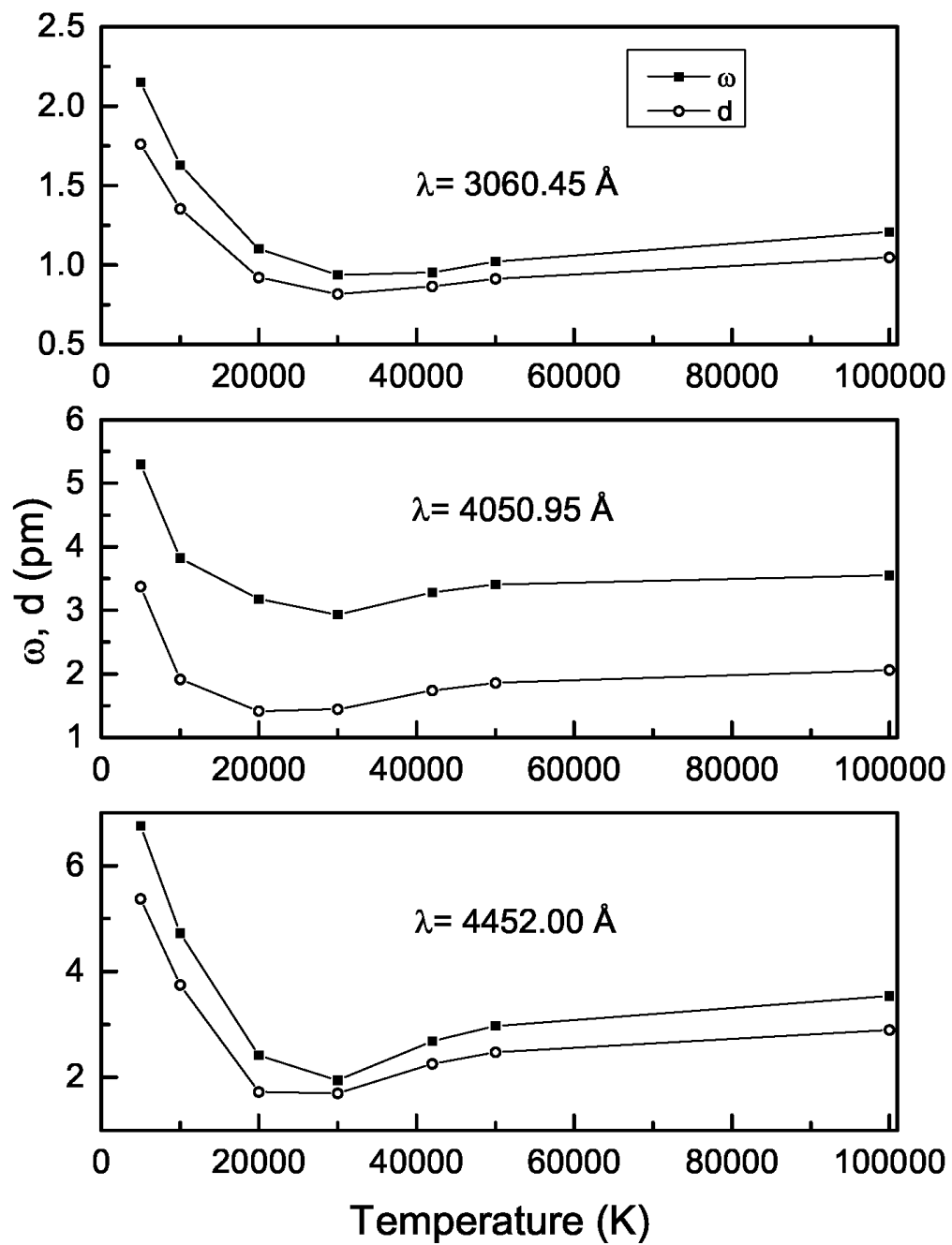


Figure 1. Calculated Stark width (full-width at half maximum (FWHM)) ω (pm), and shifts (d (pm)) normalized to $N_e = 10^{15} \text{ cm}^{-3}$ vs. temperature for spectral lines of neutral vanadium of astrophysical interest.

Table 2. Neutral vanadium (V I) line-widths (FWHM), ω (pm), and shifts (d(pm)) normalized to $Ne = 10^{15} \text{ cm}^{-3}$.

Wavelength λ (Å) ^a	Transition Levels		T (10 ³ K)	ω (pm)	d (pm)	
	Aij (10 ⁸ s ⁻¹) ^a	Upper				Lower
3056.33		3d ³ 4s4p ⁴ F _{5/2} ^o	3d ³ 4s ² 4F _{5/2}	5	1.61	-1.32
Aij = 1.33				10	1.22	-1.01
				20	0.82	-0.69
				30	0.69	-0.60
3060.45		3d ³ 4s4p ⁴ F _{7/2} ^o	3d ³ 4s ² 4F _{7/2}	5	2.15	-1.76
Aij = 1.46				10	1.63	-1.35
				20	1.10	-0.92
				30	0.94	-0.82
3207.40		3d ³ 4s4p ⁴ G _{9/2} ^o	3d ³ 4s ² 4F _{9/2}	5	2.94	-2.56
Aij = 0.218				10	2.02	-1.74
				20	1.34	-1.15
				30	0.92	-0.76
3400.39		3d ⁴ 4p ⁴ D _{7/2} ^o	3d ⁴ 4s ⁴ D _{7/2}	5	2.30	-1.78
Aij = 0.191				10	1.46	-1.0
				20	0.99	0.60
				30	1.03	-0.80
3533.67		3d ⁴ 4p ⁴ D _{7/2} ^o	3d ³ 4s ² 4P _{5/2}	5	2.39	-1.83
Aij = 0.63				10	1.51	-1.02
				20	1.19	-0.78
				30	1.09	-0.84
3667.73		3d ³ 4s4d ⁶ H _{7/2}	3d ³ 4s4p ⁶ G _{5/2} ^o	5	3.34	-2.81
Aij = 1.46				10	1.89	-1.52
				20	2.37	-2.10
				30	2.24	-2.19
3688.06		3d ³ 4s4p ⁶ P _{7/2} ^o	3d ⁴ 4s ⁶ D _{7/2}	5	2.20	-1.63
Aij = 0.32				10	1.43	-1.17
				20	1.01	-0.71
				30	0.56	-0.37
3690.27		3d ³ 4s4p ⁶ P _{3/2} ^o	3d ⁴ 4s ⁶ D _{1/2}	5	0.89	-0.60
Aij = 0.44				10	0.57	-0.43
				20	0.40	-0.25
				30	0.23	-0.14
3692.21		3d ³ 4s4p ⁶ P _{5/2} ^o	3d ⁴ 4s ⁶ D _{5/2}	5	1.47	-1.04
Aij = 0.55				10	0.95	-0.75
				20	0.67	-0.44
				30	0.39	-0.25
3695.86		3d ³ 4s4p ⁶ P _{5/2} ^o	3d ⁴ 4s ⁶ D _{7/2}	5	1.11	-0.82
Aij = 0.62				10	0.72	-0.59
				20	0.51	-0.36
				30	0.27	-0.18
3704.69		3d ³ 4s4p ⁶ P _{3/2} ^o	3d ⁴ 4s ⁶ D _{3/2}	5	1.70	-1.27
Aij = 0.77				10	1.11	-0.91
				20	0.78	-0.56
				30	0.43	-0.28
3705.03		3d ³ 4s4p ⁶ P _{3/2} ^o	3d ⁴ 4s ⁶ D _{5/2}	5	1.34	-1.05
Aij = 0.418				10	0.89	-0.75
				20	0.62	-0.47
				30	0.31	-0.21

Table 2. Cont.

Wavelength λ (Å) ^a	Transition Levels		T (10 ³ K)	ω (pm)	d (pm)	
	Aij (10 ⁸ s ⁻¹) ^a	Upper				Lower
3808.51		3d ⁴ 4p ⁴ D _{3/2} ^o	3d ⁴ 4s ⁴ F _{3/2}	5	1.54	-1.31
Aij = 0.143				10	1.01	-0.85
				20	0.68	-0.61
				30	0.61	-0.55
3823.21		3d ³ 4s4p ⁶ D _{3/2} ^o	3d ⁴ 4s ⁶ D _{5/2}	5	1.31	-1.26
Aij =0.164				10	0.91	-0.88
				20	0.60	-0.58
				30	0.21	-0.20
4050.95		3d ⁴ 4p ⁴ G _{9/2} ^o	3d ⁴ 4s ⁴ G _{9/2}	5	5.30	-3.37
Aij = 0.70				10	3.82	-1.91
				20	3.18	-1.41
				30	2.93	-1.44
4095.47		3d ³ 4s4p ⁴ F _{7/2} ^o	3d ⁴ 4s ⁴ D _{5/2}	5	3.37	-2.67
Aij = 0.42				10	2.58	-2.08
				20	1.55	-1.22
				30	1.50	-1.29
4099.78		3d ⁴ 4p ⁶ D _{7/2} ^o	3d ⁴ 4s ⁶ D _{5/2}	5	2.81	-2.18
Aij = 0.391				10	1.99	-1.54
				20	1.08	-0.76
				30	0.82	-0.73
4105.157		3d ⁴ 4p ⁶ D _{5/2} ^o	3d ⁴ 4s ⁶ D _{3/2}	5	2.03	-1.56
Aij = 0481				10	1.44	-1.10
				20	0.77	-0.53
				30	0.60	-0.53
4111.778		3d ⁴ 4p ⁶ D _{9/2} ^o	3d ⁴ 4s ⁶ D _{9/2}	5	3.92	-3.12
Aij = 1.0				10	2.77	-2.20
				20	1.55	-1.16
				30	1.11	1.0
4115.17		3d ⁴ 4p ⁶ D _{7/2} ^o	3d ⁴ 4s ⁶ D _{7/2}	5	3.11	-2.47
Aij = 0.57				10	2.20	-1.75
				20	1.22	-0.91
				30	0.87	-0.78
4116.47		3d ⁴ 4p ⁶ D _{5/2} ^o	3d ⁴ 4s ⁶ D _{5/2}	5	2.32	-1.84
Aij = 0.215				10	1.64	-1.30
				20	0.91	-0.67
				30	0.64	-0.57
4116.55		3d ⁴ 4p ⁶ D _{1/2} ^o	3d ⁴ 4s ⁶ D _{1/2}	5	0.79	-0.63
Aij = 0.276				10	0.56	-0.44
				20	0.31	-0.23
				30	0.22	-0.20
4182.58		3d ⁴ 4p ⁴ F _{7/2} ^o	3d ⁴ 4s ⁶ D _{5/2}	5	3.06	-2.40
Aij =0.012				10	2.06	-1.60
				20	1.33	-1.17
				30	1.18	-1.0
4232.45		3d ⁴ 4p ⁴ F _{9/2} ^o	3d ⁴ 4s ⁴ F _{9/2}	5	5.37	-3.47
Aij = 0.69				10	3.37	-2.37
				20	2.75	-1.50
				30	2.45	-1.34

Table 2. Cont.

Wavelength λ (Å) ^a	Transition Levels		T (10 ³ K)	ω (pm)	d (pm)	
	Aij (10 ⁸ s ⁻¹) ^a	Upper				Lower
4379.23		3d ⁴ 4p ⁶ F _{11/2} ^o	3d ⁴ 4s ⁶ D _{9/2}	5	4.82	-3.64
Aij = 1.15				10	3.41	-2.58
				20	1.75	-1.16
				30	1.27	-1.06
4400.57		3d ⁴ 4p ⁶ F _{3/2} ^o	3d ⁴ 4s ⁶ D _{1/2}	5	1.41	-1.01
Aij = 0.347				10	1.0	-0.72
				20	0.48	-0.28
				30	0.39	-0.32
4408.19		3d ⁴ 4p ⁶ F _{5/2} ^o	3d ⁴ 4s ⁶ D _{5/2}	5	2.59	2.00
Aij = 0.51				10	1.83	-1.41
				20	0.96	-0.66
				30	0.66	-0.55
4412.136		3d ⁴ 4p ⁴ P _{1/2} ^o	3d ⁴ 4s ⁶ D _{1/2}	5	0.93	-0.71
Aij = 0.0426				10	0.59	-0.44
				20	0.36	-0.33
				30	0.31	-0.23
4419.93		3d ⁴ 4p ⁶ P _{7/2} ^o	3d ⁴ 4s ⁶ D _{5/2}	5	3.10	-1.73
Aij = 0.0122				10	2.17	-1.24
				20	1.52	-0.38
				30	1.15	-0.06
4421.56		3d ⁴ 4p ⁶ F _{3/2} ^o	3d ⁴ 4s ⁶ D _{5/2}	5	2.06	-1.66
Aij = 0.133				10	1.46	-1.17
				20	0.80	-0.60
				30	0.50	-0.42
4437.83		3d ⁴ 4p ⁶ P _{7/2} ^o	3d ⁴ 4s ⁶ D _{7/2}	5	3.45	-2.06
Aij = 0.0836				10	2.42	-1.48
				20	1.69	-0.54
				30	1.21	-0.11
4444.20		3d ⁴ 4p ⁶ P _{3/2} ^o	3d ⁴ 4s ⁶ D _{3/2}	5	1.50	-1.29
Aij = 0.148				10	1.23	-0.74
				20	0.85	-0.27
				30	0.62	-0.06
4452.00		3d ⁴ 4p ⁴ I _{15/2} ^o	3d ⁴ 4s ⁴ H _{13/2}	5	6.75	-5.37
Aij = 0.81				10	4.72	-3.75
				20	2.42	-1.72
				30	1.94	-1.70
4468.00		3d ⁴ 4p ⁴ I _{9/2} ^o	3d ⁴ 4s ⁴ H _{7/2}	5	3.97	-3.11
Aij = 0.174				10	2.78	-2.18
				20	1.39	-0.97
				30	1.16	-1.0
4560.71		3d ⁴ 4p ⁴ G _{9/2} ^o	3d ⁴ 4s ⁴ F _{7/2}	5	4.0	-3.09
Aij = 0.58				10	2.80	-2.15
				20	1.39	-0.96
				30	1.07	-0.88

Note. A negative shift is towards the red, ^aNIST.

4. Conclusions

In this work, we presented theoretical Stark broadening parameters of 35 spectral lines of V I of astrophysical and industrial interest in the ultraviolet–blue range. It is the first time that these values, for which there are no experimental measurements, have been calculated. To get the required matrix elements, we used the transition probabilities obtained from Cowan’s code (around 190,000). The theoretical lifetimes of the upper levels of these transitions are also shown.

Author Contributions: Conceptualization: C.C., M.I.d.A.-G., L.I.-G., and A.M.; Methodology: C.C., M.I.d.A.-G., L.I.-G., and A.M.; Investigation: C.C., M.I.d.A.-G., L.I.-G., and A.M.; Writing—review and editing: C.C. and L.I.-G. All authors have read and agreed to the published version of the manuscript.

Funding: This research received no external funding.

Acknowledgments: This work was financially supported by the Spanish DGI project MAT2015- 63974-C4-2-R.

Conflicts of Interest: The authors declare no conflict of interest.

References

1. Woosley, S.E.; Weaver, A.T. The Evolution and Explosion of Massive Stars. II. Explosive Hydrodynamics and Nucleosynthesis. *Rev. Mod. Phys.* **1995**, *101*, 181.
2. Ou, X.; Roederer, I.U.; Sneden, C.; Cowan, J.J.; Lawler, J.E.; Shectman, S.A.; Thompson, I.B. Vanadium Abundance Derivations in 255 Metal-poor Stars. *arXiv* **2020**, arXiv:2008.05500.
3. Cowan, J.J.; Sneden, C.; Roederer, I.U.; Lawler, J.E.; Hartog, E.A.D.; Sobeck, J.S.; Boesgaard, A.M. Detailed Iron-peak Element Abundances in Three Very Metal-poor Stars. *Astrophys. J.* **2020**, *890*, 119. [[CrossRef](#)]
4. Manrique, J.; Pace, D.M.D.; Aragón, C.; Aguilera, J.A. Experimental Stark widths and shifts of V II spectral lines. *Mon. Not. R. Astron. Soc.* **2020**. [[CrossRef](#)]
5. Lawler, J.E.; Wood, M.P.; Hartog, E.A.D.; Feigenson, T.; Sneden, C.; Cowan, J.J. Improved V I log(gf) values and abundance determinations in the photospheres of the sun and metal-poor star hd 84937. *Astrophys. J. Suppl. Ser.* **2014**, *215*, 20. [[CrossRef](#)]
6. Scott, P.; Asplund, M.; Grevesse, N.; Bergemann, M.; Jacques Sauval, A. The elemental composition of the Sun-II. The iron group elements Sc to Ni. *Astron. Astrophys.* **2015**, *573*, A26. [[CrossRef](#)]
7. Wood, M.P.; Sneden, C.; Lawler, J.E.; Hartog, E.A.D.; Cowan, J.J.; Nave, G. Vanadium Transitions in the Spectrum of Arcturus. *Astrophys. J. Suppl. Ser.* **2018**, *234*, 25. [[CrossRef](#)]
8. Moore, C.E. *Atomic Energy Levels*; NBS 467-11C; U.S.GPO: Washington, DC, USA, 1958.
9. Sugar, P.; Corliss, C. Atomic Energy Levels of the Iron-Period Elements: Potassium through Nickel. *J. Phys. Chem. Ref. Data* **1985**, *14* (Suppl. 2), 203.
10. Palmeri, P.; Biemont, E.; Aboussaid, A.; Godefroid, M. Hyperfine structure of infrared vanadium lines. *J. Phys. B At. Mol. Opt. Phys.* **1995**, *28*, 3741–3752. [[CrossRef](#)]
11. Palmeri, P.; Biémont, E.; Quinet, P.; Dembczyński, J.; Szawiola, G.; Kurucz, R.L. Term analysis and hyperfine structure in neutral vanadium. *Phys. Scr.* **1997**, *55*, 586–598. [[CrossRef](#)]
12. Lefèbvre, P.H.; Garnir, H.P.; Biémont, E. Hyperfine Structure of Neutral Vanadium Lines and Levels. *Phys. Scr.* **2002**, *66*, 363–366. [[CrossRef](#)]
13. Thorne, A.P.; Pickering, J.C.; Semeniuk, J. The spectrum and term analysis of V I. *Astrophys. J. Suppl. Ser.* **2010**, *192*, 11. [[CrossRef](#)]
14. Saloman, E.B.; Kramida, A. Critically Evaluated Energy Levels, Spectral Lines, Transition Probabilities, and Intensities of Neutral Vanadium (V i). *Astrophys. J. Suppl. Ser.* **2017**, *231*, 18. [[CrossRef](#)]
15. Hartog, E.A.D.; Lawler, J.E.; Wood, M.P. Radiative lifetimes of V I and V II. *Astrophys. J. Suppl. Ser.* **2014**, *215*, 7. [[CrossRef](#)]
16. Wang, Q.; Jiang, L.Y.; Quinet, P.; Palmeri, P.; Zhang, W.; Shang, X.; Tian, Y.S.; Dai, Z.W. TR-LIF lifetime measurements and HFR+CPOL calculations of radiative parameters in vanadium atom (V I). *Astrophys. J. Suppl. Ser.* **2014**, *211*, 31. [[CrossRef](#)]
17. Holmes, C.E.; Pickering, J.C.; Ruffoni, M.P.; Blackwell-Whitehead, R.; Nilsson, H.; Engström, L.; Hartman, H.; Lundberg, H.; Belmonte, M.T. Experimentally measured radiative lifetimes and oscillator strengths in neutral vanadium. *Astrophys. J. Suppl. Ser.* **2016**, *224*, 35. [[CrossRef](#)]

18. Kramida, A.; Ralchenco, Y.; Reader, J. NIST ASD Team (2013) NIST Atomic Spectra Database (v.5.3). 2013. Available online: <http://physics.nist.gov/asd> (accessed on 20 August 2020).
19. Sahal-Brechot, S.; Dimitrijevic, M.; Nessib, N.B.; Moreau, N. STARK-B. 2020. Available online: <http://stark-b.obspm.fr/index.php/contact> (accessed on 20 August 2020).
20. Iqbal, A.; Suhaimi, H.; Zhao, W.; Jamil, M.; Nauman, M.M.; He, N.; Zaini, J. Sustainable Milling of Ti-6Al-4V: Investigating the Effects of Milling Orientation, Cutter's Helix Angle, and Type of Cryogenic Coolant. *Metals* **2020**, *10*, 258. [[CrossRef](#)]
21. Carreón, H.; Barriuso, S.; González, J.A.P.; González-Carrasco, J.L.; Moreno, J.L.O. Thermoelectric assessment of laser peening induced effects on a metallic biomedical Ti6Al4V. In Proceedings of the Frontiers in Ultrafast Optics: Biomedical, Scientific, and Industrial Applications XIV, San Francisco, CA, USA, 2–5 February 2014; SPIE: Bellingham WA, USA, 2014; Volume 8972, pp. 89721Q-1–89721Q-7.
22. De Andrés García, M.I. Utilización de la línea H α del hidrógeno en la caracterización de los plasmas generados por láser para aplicaciones industriales (técnicas LSP) y espectroscópicas. Ph.D. Thesis, ETSIDI, Madrid, Spain, 2017. doi:10.20868/UPM.thesis.47301. [[CrossRef](#)]
23. Griem, H.T. Semiempirical formulas for the Electron-Impact widths and shifts of isolated ion lines in plasmas. *Phys. Rev.* **1968**, *165*, 258–266. [[CrossRef](#)]
24. Baranger, M. General Impact Theory of Pressure Broadening*. *Phys. Rev.* **1958**, *112*, 855–865. [[CrossRef](#)]
25. Seaton, M.J. The Theory of Excitation and Ionization by Electron Impact. In *Proceedings of the Atomic and Molecular Processes*; Bates, D.R., Ed.; Elsevier: Amsterdam, The Netherlands, 1962.
26. Van Regemorter, H. Rate of Collisional Excitation in Stellar Atmospheres. *Astrophys. J.* **1962**, *136*, 906. [[CrossRef](#)]
27. Cowan, R. *The Theory of Atomic Structure and Spectra*; University of California Press: Berkeley, CA, USA, 1981; p. 57. [[CrossRef](#)]



© 2020 by the authors. Licensee MDPI, Basel, Switzerland. This article is an open access article distributed under the terms and conditions of the Creative Commons Attribution (CC BY) license (<http://creativecommons.org/licenses/by/4.0/>).